DOI: 10.1021/ic100996b

Inorganic Chemistry
Article

Mechanistic Insight into the Alcohol Oxidation Mediated by an Efficient Green [$CuBr_2$(2,2′-bipy)]-TEMPO Catalyst by Density Functional Method

Lin Cheng,[†] Jinping Wang,[‡] Meiyan Wang,[†] and Zhijian Wu*[,†]

[†]*State Key Laboratory of Rare Earth Resource Utilization, Changchun Institute of Applied Chemistry, Chinese Academy of Sciences, Changchun 130022, P.R. China, and* [‡]*Department of Applied Chemistry, Qingdao Agricultural University, Qingdao 266109, P. R. China*

Received May 19, 2010

Density functional theory (DFT) calculations have been performed to investigate the alcohol oxidation to acetaldehyde catalyzed by [$CuBr_2$(2,2′-bipy)]-TEMPO (TEMPO stands for 2,2,6,6-tetramethylpiperidinyloxy; bipy stands for bipyridine). The total charge for the studied catalytic system is +1. The catalytic cycle consists of two parts, namely, alcohol oxidation and TEMPO regeneration. In alcohol oxidation, the reaction follows the Sheldon's mechanism for the proposed two mechanisms, i.e., Semmelhack's mechanism and Sheldon's mechanism. The water participation plays minor role in the H atom abstraction step. In TEMPO regeneration, the proposed three paths are competitive in energy. By comparing with experimental observation, it is found that the path, in which alcohol provides the proton to $TEMPO^-$ to produce TEMPOH followed by the oxidation of TEMPOH directly to TEMPO by O_2, is favored. In TEMPO regeneration, CH_3CN acts as the ligand to stabilize the Cu^I species during the catalytic cycle.

Introduction

Selective catalytic oxidation of alcohol is one of the most attractive transformations in the modern organic synthesis and chemical industry.[1] Unfortunately, the alcohol oxidation is often accompanied by toxic stochiometric oxidations and forcing conditions, e.g., chromium(VI) oxide,[2d] dichromate,[2e] and ruthenium (VIII) oxide,[2h] which are generally toxic and produce a large amount of waste. Consequently, from an environmental and economic point of view, it is demanding to develop new and green oxidation method to replace the traditional stoichiometric oxidation.

In recent years, much attention for the alcohol oxidation has been focused on the development of metal based catalysts using clean oxidants, e.g., air, oxygen, or H_2O_2. It is well-known that the galactose oxidase (GOase) could selectively transforms primary alcohols in the presence of O_2 to aldehydes and H_2O_2.[3] Thus, a vast number of copper complexes have been synthesized as the functional models of GOase such as those by the groups of Stack[4] and Wieghardt.[5] Stack group obtained a [Cu(II)BSP] species,[4a] which is able to catalyze the oxidation of benzylic and allylic alcohols under dioxygen at room temperature. Wieghardt group developed the catalytic oxidation of primary and secondary alcohols by a dinuclear Cu(II)−phenoxyl complex at 20 °C.[5a] However, the catalytic activities for the most of these synthetic models are low, and most of them can only oxidize the active alcohol. On the other hand, a series of TEMPO based (TEMPO stands for 2,2,6,6-tetramethylpiperidinyloxy) copper systems have also been reported to be potential environmental benign catalysts.[6] The stable, nonconjugated nitroxyl

*Corresponding author. Fax: +86-431-85698041. E-mail: zjwu@ciac.jl.cn.

(1) (a) *Transition Metals for Organic Synthesis*; Beller, M., Bolm, C., Eds.; Wiley-VCH: Weinheim, Germany, 1998; Vol. *2*, p 350. (b) Sheldon, R. A.; Kochi, J. K. *Metal-Catalyzed Oxidations of Organic Compounds*; Academic Press: New York, 1981. (c) *Comprehensive Organic Synthesis*; Trost, B. M.; Fleming, I.; Ley, S. V.; Eds.; Pergamon: Oxford, 1991; Vol. *7*, pp 251. (d) Cainelli, G.; Cardillo, G. *Chromium Oxidations in Organic Chemistry*; Springer: Berlin, 1984.

(2) (a) *Ullman's Encyclopedia of Industrial Chemistry*, 6th ed.; Wiley-VCH: Weinheim, Germany, 2002. (b) *Principles of Organic Synthesis*, 3rd ed.; Blackie Academic & Proffesional, London, 1993. (c) Stevens, R. V.; Chapman, K. T.; Weller, H. N. *J. Org. Chem.* **1980**, *45*, 2030. (d) Holum, J. R. *J. Org. Chem.* **1961**, *26*, 4814. (e) Lee, D. G.; Spitzer, U. A. *J. Org. Chem.* **1970**, *35*, 3589. (f) Highet, R. J.; Wildman, W. C. *J. Am. Chem. Soc.* **1955**, *77*, 4399. (g) Menger, F. M.; Lee, C. *Tetrahedron Lett.* **1981**, *22*, 1655. (h) Berkowitz, L. M.; Rylander, P. N. *J. Am. Chem. Soc.* **1958**, *80*, 6682.

(3) (a) Whittaker, J. W. In *Metalloenzymes Involving Amino Acid Residues and Related Radicals*; Sigel, H., Sigel, A., Eds.; Marcel Dekker: New York, 1994; Vol. *30*, p 315. (b) Knowles, P. F.; Ito, N. In *Perspectives in Bio-inorganic Chemistry*; Jai Press: London, 1994; Vol. *2*, p 207.

(4) (a) Wang, Y.; DuBois, J. L.; Hedman, B.; Hodgson, K. O.; Stack, T. D. P. *Science* **1998**, *279*, 537. (b) Mahadevan, V.; Gebbink, R. J. M. K.; Stack, T. D. P. *Curr. Opin. Chem. Biol.* **2000**, *4*, 228. (c) Wang, Y.; Stack, T. D. P. *J. Am. Chem. Soc.* **1996**, *118*, 13097. (d) Mahadevan, V.; DuBois, J. L.; Hedman, B.; Hodgson, K. O.; Stack, T. D. P. *J. Am. Chem. Soc.* **1999**, *121*, 5583.

(5) (a) Chaudhuri, P.; Hess, M.; Flörke, U.; Wieghardt, K. *Angew. Chem., Int. Ed.* **1998**, *37*, 2217. (b) Chaudhuri, P.; Hess, M.; Weyhermüller, T.; Wieghardt, K. *Angew. Chem., Int. Ed.* **1999**, *38*, 1095. (c) Chaudhuri, P.; Hess, M.; Muller, J.; Hildenbrand, K.; Bill, E.; Weyhermuller, T.; Wieghardt, K. *J. Am. Chem. Soc.* **1999**, *121*, 9599.

(6) (a) Sheldon, R. A.; Arends, I. W. C. E.; Brink, G-J. T.; Dijksman, A. *Acc. Chem. Res.* **2002**, *35*, 774. (b) Figiel, P. J.; Leskelä, M.; Repo, T. *Adv. Synth. Catal.* **2007**, *349*, 1173. (c) Lu, Z. L.; Costa, J. S.; Roubeau, O.; Mutikainen, I.; Turpeinen, U.; Teat, S. J.; Gamez, P.; Reedijk, J. *Dalton. Trans.* **2008**, 3567. (d) Jiang, N.; Ragauskas, A. J. *J. Org. Chem.* **2006**, *71*, 7087.

Published on Web 09/17/2010

radical TEMPO can be stored for a long time without decomposition.[7] The CuCl−TEMPO system was first reported by Semmelhack and co-workers.[8] A mechanism was proposed in which one-electron oxidation of TEMPO by Cu(II) gives the oxoammonium cation. More recently, the Sheldon group has investigated the mechanism proposed by Semmelhack and co-workers and developed a new catalytic mechanism.[9] Furthermore, they reported an efficient Cu^{II}/bipyridine-TEMPO catalytic system.[10] Typically, the alcohol oxidation was carried out by Cu^{II}/bipyridine-TEMPO system in an acetonitrile/water (2:1) solvent mixture at room temperature. Moreover, it is important to note that after the oxidation reaction, the copper catalyst is still active. Adding one more equivalent of benzyl alcohol and another 5 mol % TEMPO to the reaction mixture could continue the oxidation reaction. Therefore, this catalytic system turns out to be a very attracting catalytic system from both economic and environmental point of view. Moreover, an interesting phenomenon was observed, i.e., the concentration of TEMPO is constant during the course of the reaction and dramatically drops when all the substrate is consumed, which could not be explained experimentally.[10]

In this work, we present density functional theory (DFT) calculations on the catalytic reaction mechanism of the Cu-TEMPO catalytic system. The catalytic cycle of Cu-TEMPO system consists of two parts, namely, alcohol oxidation and TEMPO regeneration. For the alcohol oxidation, two mechanisms were proposed, e.g., Semmelhack's mechanism (oxoammonium cation as the oxidant)[8] and Sheldon's mechanism (copper-centered oxidative dehydrogenation of the alcohol).[9] Recently, Baerend group[11] have studied the alcohol oxidation by the OPBE functional[12] with a basis set of Slater-type orbitals of TZP quality. From that study, only the restricted singlet species Cu-TEMPO was obtained as the starting structure. Thus, they indicated that the mechanism for the alcohol oxidation follows the Semmelhack's mechanism. In this work, by re-examining the starting structure, we have found that besides the restricted singlet species Cu-TEMPO, the open shell singlet and triplet spin states are also obtained. Our calculations indicate that restricted singlet state is 10.9 and 6.7 kcal/mol higher in energy than the open shell singlet and triplet spin states in solution. Thus, open shell state is more suitable to be the starting structure. In addition, by choosing the restricted singlet state as the starting structure, we have reproduced the mechanism studied by Baerend and co-workers.[11] On the other hand, we have also studied the TEMPO regeneration, which is not accessed by Baerend and co-workers.[11]

Computational Methods

The calculations were performed by use of the Gaussian 03 suite of programs.[13] In the model reaction, the substrate benzyl alcohol was simplified to methanol, and the four methyl groups in TEMPO have been replaced by H atoms. Geometries of the stationary points on the energy profiles were optimized by use of B3LYP functional and the standard 6-31G(d) basis set.[14] The same level of theory was used for calculating Hessians and thermal corrections. Relative free energies were obtained by performing single point calculations at B3LYP/6-311+G(d,p) and by including thermal corrections to free energies at B3LYP/6-31G(d), which includes entropy contributions by taking into account the vibrational, rotational and translational motions of the species at 298.15 K. The stationary points and transition states on the energy profiles were confirmed by the normal-mode analysis. Spin densities (ρ) are reported by Mulliken population analysis from larger basis set (6-311+G(d,p)) calculations. All the complexes in the open shell singlet state were calculated by the symmetry-broken method as used by Wieghardt group.[15] Many open shell calculations for antiferromagnetic coupled singlet state result in a great degree of spin contamination with $\langle S^2\rangle_S$ in the range of 0.26−1.00 (0 for pure singlet). This large spin contamination will result some errors in the description of the open shell singlet state. Thus, the energy correction was estimated from the Heisenberg spin-Hamiltonian formalism.[16] The energy correction can be estimated from the following equation:

$$\Delta_{ST} = 2(E_S - E_T)/(2 - \langle S^2\rangle_S)$$

where E_S is the open shell singlet energy, E_T is the triplet energy, $\langle S^2\rangle_S$ is the spin contamination for the open shell singlet. Subscript S subscript stands for open shell singlet, T for triplet. This energy correction approach has been widely used in the previous studies.[15,17] The intrinsic reaction coordinate (IRC) approach was used to confirm that the transition state connects the two relevant minima.[18] The solvent effect on the potential energy surface was investigated by single point calculations at B3LYP/6-311+G(d,p) level with the conductor-like polarized continuum solvent model (CPCM)[19] using the acetonitrile/water (2:1) (ε = 50.6) as the solvent.[20]

(7) Sheldon, R. A.; Arends, I. W. C. E. *Adv. Synth. Catal.* **2004**, *346*, 1051.
(8) Semmelhack, M. F.; Schmid, C. R.; Cortés, D. A.; Chou, C. S. *J. Am. Chem. Soc.* **1984**, *106*, 3374.
(9) Dijksman, A.; Arends, I.; Sheldon, R. A. *Org. Biomol. Chem.* **2003**, *1*, 3232.
(10) (a) Gamez, P.; Arends, I. W. C. E.; Reedijk, J.; Sheldon, R. A. *Chem. Commun.* **2003**, 2414. (b) Gamez, P.; Arends, I. W. C. E.; Sheldon, R. A.; Reedijk, J. *Adv. Synth. Catal.* **2004**, *346*, 805.
(11) Michel, C.; Belanzoni, P.; Gamez, P.; Reedijk, J.; Baerends, E. J. *Inorg. Chem.* **2009**, *48*, 11909.
(12) (a) Cohen, A. J.; Handy, N. C. *Mol. Phys.* **2001**, *99*, 607. (b) Perdew, J.; Burke, K.; Ernzerhof, M. *Phys. Rev. Lett.* **1996**, *77*, 3865.
(13) Frisch, M. J.; Trucks, G. W.; Schlegel, H. B.; Scuseria, G. E.; Robb, M. A.; Cheeseman, J. R.; Montgomery, J. A., Jr.; Vreven, T.; Kudin, K. N.; Burant, J. C.; Millam, J. M.; Iyengar, S. S.; Tomasi, J.; Barone, V.; Mennucci, B.; Cossi, M.; Scalmani, G.; Rega, N.; Petersson, G. A.; Nakatsuji, H.; Hada, M.; Ehara, M.; Toyota, K.; Fukuda, R.; Hasegawa, J.; Ishida, M.; Nakajima, T.; Honda, Y.; Kitao, O.; Nakai, H.; Klene, M.; Li, X.; Knox, J. E.; Hratchian, H. P.; Cross, J. B.; Adamo, C.; Jaramillo, J.; Gomperts, R.; Stratmann, R. E.; Yazyev, O.; Austin, A. J.; Cammi, R.; Pomelli, C.; Ochterski, J. W.; Ayala, P. Y.; Morokuma, K.; Voth, G. A.; Salvador, P.; Dannenberg, J. J.; Zakrzewski, V. G.; Dapprich, S.; Daniels, A. D.; Strain, M. C.; Farkas, O.; Malick, D. K.; Rabuck, A. D.; Raghavachari, K.; Foresman, J. B.; Ortiz, J. V.; Cui, Q.; Baboul, A. G.; Clifford, J.; Cioslowski, J.; Stefanov, B. B.; Liu, G.; Liashenko, A.; Piskorz, P.; Komaromi, I.; Martin, R. L.; Fox, D. J.; Keith, T.; Al-Laham, M. A.; Peng, C. Y.; Nanayakkara, A.; Challacombe, M.; Gill, P. M. W.; Johnson, B.; Chen, W.; Wong, M. W.; Gonzalez, C.; Pople, J. A. *Gaussian 03*; Gaussian, Inc.: Pittsburgh, PA, 2003.
(14) (a) Becke, A. D. *J. Chem. Phys.* **1993**, *98*, 5648. (b) Lee, C.; Yang, W.; Parr, R. G. *Phys. Rev. B.* **1988**, *37*, 785. (c) Becke, A. D. *Phys. Rev. A.* **1988**, *38*, 3098.
(15) Bachler, V.; Olbrich, G.; Neese, F.; Wieghardt, K. *Inorg. Chem.* **2002**, *41*, 4179.
(16) (a) Mouesca, J. M.; Chen, J. L.; Noodleman, L.; Bashford, D.; Case, D. A. *J. Am. Chem. Soc.* **1994**, *116*, 11898. (b) Noodleman, L. *J. Chem. Phys.* **1981**, *74*, 5737. (c) Ciofini, L.; Daul, C. A. *Coord. Chem. Rev.* **2003**, *238*−*239*, 187.
(17) (a) Cheng, L.; Wang, J. P.; Wang, M. Y.; Wu, Z. J. *Dalton. Trans.* **2009**, 3286. (b) Bachler, V.; Chaudhuri, P.; Wieghardt, K. *Chem.—Eur. J.* **2001**, *7*, 404. (c) Siegbahn, P. E. M.; Pelmenschikov, V. *J. Am. Chem. Soc.* **2006**, *128*, 7466.
(18) (a) Fukui, K. *Acc. Chem. Res.* **1981**, *14*, 363. (b) Fukui, K. *J. Phys. Chem.* **1970**, *74*, 4161.
(19) (a) Barone, V.; Cossi, M. *J. Phys. Chem. A.* **1998**, *102*, 1995. (b) Cossi, M.; Scalmani, G.; Rega, N.; Barone, V. *J. Comput. Chem.* **2003**, *24*, 669.
(20) Al-Qunaibit, M. H. *Bioinorg. Chem. Appl.* **2009**10.1155/2009/561091.

Scheme 1. Proposed Catalytic Mechanisms for the Alcohol Oxidation

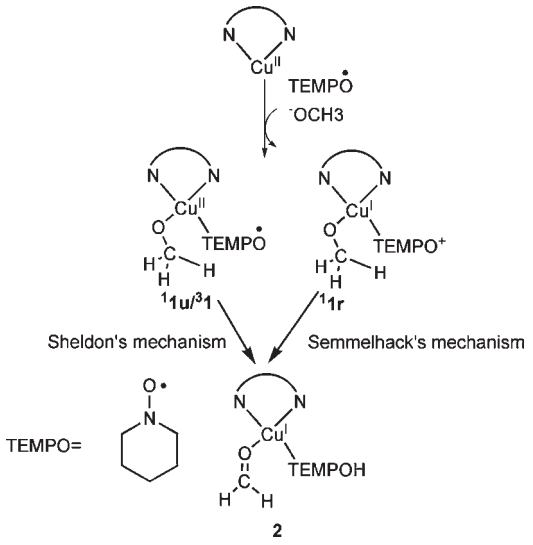

Although B3LYP is demonstrated to give good results for the Cu complexes,[21] the MPW1P95[22] functional was also adopted for comparison. The energies are all in kcal/mol.

Results and Discussion

1. Alcohol Oxidation. 1.1. Starting Structures. The proposed mechanisms of the Cu-TEMPO catalyzed alcohol oxidation reaction were presented in Scheme 1. Experimental study indicated that the substrate alcohol is probably deprotonated to alkoxide ($^-OCH_3$) by the basic cocatalyst (potassium hydroxide).[10] Thus, we propose that $^-OCH_3$ and TEMPO are coordinated to the Cu^{II} ion of the Cu^{II}-bipy complex to initiate the alcohol oxidation. Then, the complex ($^-OCH_3$)Cu^{II}(TEMPO)-(bipy) (denoted as **1**) is the reasonable starting structure for the alcohol oxidation. Similar situation was encountered in the previous mechanistic study of GOase functional complex.[23] From **1**, two possible mechanisms have been proposed (Scheme 1), i.e., Semmelhack's mechanism[8] and Sheldon's mechanism.[9] In Sheldon's mechanism, **1** has the Cu^{II}-TEMPO character. On the contrary, **1** has the Cu^{I}-$TEMPO^+$ character in Semmelhack's mechanism. In principle, the unpaired electrons of Cu^{II} (d^9, S_{Cu} = 1/2) and of TEMPO (S = 1/2) in **1** can be antiferromagnetically and ferromagnetically coupled yielding the open shell singlet ^{1}**1u** and triplet state ^{3}**1**. In addition, the unpaired electron of the TEMPO radical migrating to the Cu^{II} ion could produce closed shell singlet state **1** with Cu^{I}-$TEMPO^+$ character. For **1**, geometry optimizations were performed by considering three possible isomers (η^1-*O*-bound, η^1-*N*-bound or η^2-*O*,*N*-bound) in three spin states. In our calculations, the η^1-*N*-bound and η^2-*O*,*N*-bound isomers converged to the η^1-*O*-bound isomer during the optimization process. This is consistent with the situation for the TEMPO coordination to Cu, Ru, and Ir.[11,24] For ^{1}**1u** (^{3}**1**), the calculated spin densities on Cu, TEMPO group, methoxyl group and bipy ligand are 0.51 (0.56), −0.81 (1.00), 0.17 (0.21), and 0.13 (0.23), respectively (negative sign indicates the opposite direction). For ^{1}**1r**, the spin density of each atom is zero. From the previous study on the Cu-containing enzyme by Siegbahn,[25] Cu is assigned to be Cu(II) state when the spin density is around 0.50, Cu(I) state when the spin density is 0.0, mixture of Cu(I) and Cu(II) when the spin density is in the range 0.20−0.30. Moreover, for ^{1}**1u**, electronic configuration is the combination of $d^2_{yz}d^2_{z2}d^2_{xz}d^2_{xy}d^1_{x^2-y^2}$ antiferromagnetically coupled with the β-spin unpaired electron on TEMPO. This is further supported by the molecular orbitals for ^{1}**1u** (Scheme 2). It is seen that the two unpaired electrons are located in a TEMPO π-type orbital and Cu $d_{x^2-y^2}$ orbital with a significant contribution of the σ orbital of the connecting atoms, respectively. ^{1}**1u** has a weak antiferromagnetic coupling character between Cu and TEMPO. For ^{3}**1**, electronic configuration is the combination of $d^2_{yz}d^2_{z2}d^2_{xz}d^2_{xy}d^1_{x^2-y^2}$ ferromagnetically coupled with the β-spin unpaired electron on TEMPO. Thus, combination of the electronic configuration and the spin density distributions indicate that ^{3}**1** and ^{1}**1u** possess the (bipy)Cu^{II}(TEMPO) character. Consequently, ^{3}**1** and ^{1}**1u** could be the starting structure for the Sheldon's mechanism. For ^{1}**1r**, if it has the Cu^{I}-$TEMPO^+$ character, it could be the starting structure for the Semmelhack's mechanism. However, from the NBO analysis, the atomic net charges of the nitroxide ligand in ^{1}**1r** are the same as those in the free radical: i.e., −0.04e on N and −0.44e on O in TEMPO. On the contrary, the atomic net charges of the nitroxide ligand are 0.27e on N and −0.14e on O in $TEMPO^+$. Moreover, the overall charges of TEMPO group in ^{1}**1r** is only +0.16e, which is much smaller than +1.00e. In addition, the N−O bond length of TEMPO group in ^{1}**1r** is 1.299 Å (close to that in TEMPO radical species, 1.283 Å), which is much longer than that in $TEMPO^+$ species (1.196 Å). Thus, it is obvious that the TEMPO group in ^{1}**1r** does not have the $TEMPO^+$ character. Moreover, our calculations indicated that ^{1}**1r** is 10.9 and 6.7 kcal/mol higher in energy than ^{1}**1u** and ^{3}**1** in solution, respectively. Calculations from MPW1P95 support the results from the B3LYP, in which ^{1}**1r** is 16.8 and 14.2 kcal/mol higher in energy than ^{1}**1u** and ^{3}**1** in solution, respectively. Thus, from both the NBO analysis and energy, the complex **1** (η^1-*O*-bound) will have the Cu^{II}-TEMPO character. Therefore, Semmelhack's mechanism can be excluded. On the other hand, a η^2-*O*,*N*-bound $CuBr_2$-TEMPO complex was found to have the Cu^{I}-$TEMPO^+$ character theoretically.[26a] Experimentally, however, the $CuBr_2$-TEMPO complex has the Cu^{II}-TEMPO character based on the structural parameters.[26b]

(21) (a) Guell, M.; Luis, J. M.; Siegbahn, P. E. M.; Sola, M. *J. Biol. Inorg. Chem.* **2009**, *14*, 273. (b) Latifi, R.; Bagherzadeh, M.; Milne, B. F.; Jaspars, M.; de Visser, S. P. *J. Inorg. Biochem.* **2008**, *102*, 2171. (c) Kamachi, T.; Kihara, N.; Shiota, Y.; Yoshizawa, K. *Inorg. Chem.* **2005**, *44*, 4226. (d) Prabhakar, R.; Siegbahn, P. E. M. *J. Phys. Chem. B* **2004**, *108*, 13882. (e) Siegbahn, P. E. M. *J. Biol. Inorg. Chem.* **2003**, *8*, 577. (f) Yoshizawa, K.; Shiota, Y. *J. Am. Chem. Soc.* **2006**, *128*, 9873. (g) Schröder, D.; Holthausen, M. C.; Schwarz, H. *J. Phys. Chem. B* **2004**, *108*, 14407.
(22) Zhao, Y.; Truhlar, D. G. *J. Phys. Chem. A* **2004**, *108*, 6908.
(23) Zueva, E.; Walton, P. H.; McGrady, J. E. *Dalton. Trans.* **2006**, 159.
(24) (a) Hetterscheid, D. G. H.; Kaiser, J.; Reijerse, E.; Peters, T. P. J.; Thewissen, S.; Blok, A. N. J.; Smits, J. M. M.; de Gelder, R.; de Bruin, B. *J. Am. Chem. Soc.* **2005**, *127*, 1895. (b) Chan, K. S.; Li, X. Z.; Dzik, W. I.; de Bruin, B. *J. Am. Chem. Soc.* **2008**, *130*, 2051.
(25) Siegbahn, P. E. M. *J. Biol. Inorg. Chem.* **2003**, *8*, 567.
(26) (a) Rohmer, M. M.; Grand, A; Benard, M. *J. Am. Chem. Soc.* **1990**, *112*, 2875. (b) Caneschi, A.; Grand, A.; Laugier, J.; Rey, P.; Subra, R. *J. Am. Chem. Soc.* **1988**, *110*, 2307.

Scheme 2. Molecular Orbital Energy Diagram for ^{1}**1u**. (Contour Values = ±0.04)

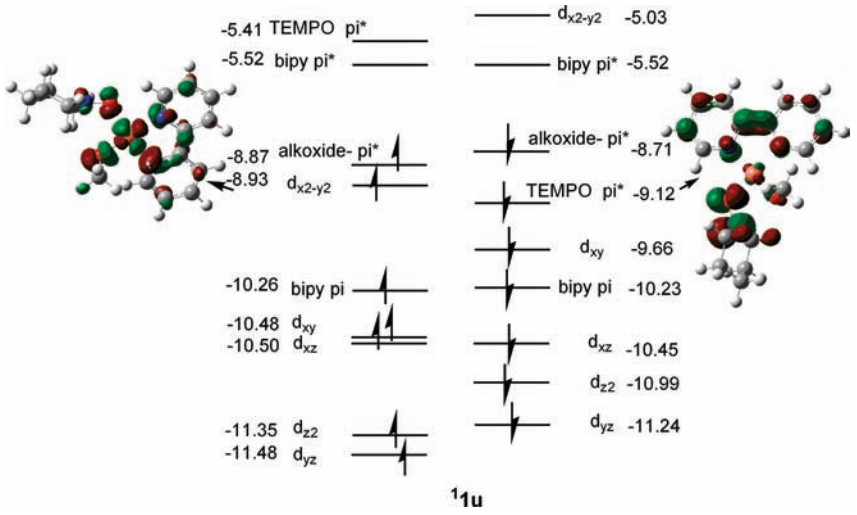

Because methanol was used as the substrate model in our calculations, different from the study of Baerend and co-workers,[11] in which propanol was used as the substrate model, we have checked the propanol as the substrate for **1** at the three spin states on the B3LYP level. Our calculations indicate that ^{1}**1r** is 10.7 and 4.6 kcal/mol higher in energy than ^{1}**1u** and ^{3}**1** in solution for the propanol model, in agreement with the results from the methanol model (^{1}**1r** is 10.9 and 6.7 kcal/mol higher in energy than ^{1}**1u** and ^{3}**1** in solution). Thus, the methanol model represents a good trade-off between accuracy and computational cost.

1.2. Substrate Oxidation. Because ^{1}**1u** is lower in energy than ^{3}**1** by 4.2 kcal/mol in solution, within the overall average error of 3−5 kcal/mol for B3LYP method,[27] the open shell singlet state (^{1}**1u**) could not be regarded as the ground state. As a consequence, the catalytic reaction mediated by the Cu-TEMPO catalyst would involve two-state reactivity (TSR).[28] The TSR is encountered in many reactions in the organometallic chemistry, especially for the Cu (ref 21.) and Fe (ref 29.) complexes. Furthermore, in order to compare with Baerend's work,[11] the reaction mechanism starting with the closed shell singlet state in the substrate oxidation is also considered.

As seen in Figure 1, the open shell singlet state is the ground state in the process **1** → **2**, similar to a previous study for galactose oxidase.[30] In this process, the H atom abstraction occurs via ^{1}**TS$_{1u-2r}$** with the energy barrier of 19.6 kcal/mol with respect to ^{1}**1u**. Thus, the H atom abstraction step is the rate-determining step. From the turnover frequency (K = 14 h^{-1}) reported experimentally,[10a] the experimental barrier height ΔG can be

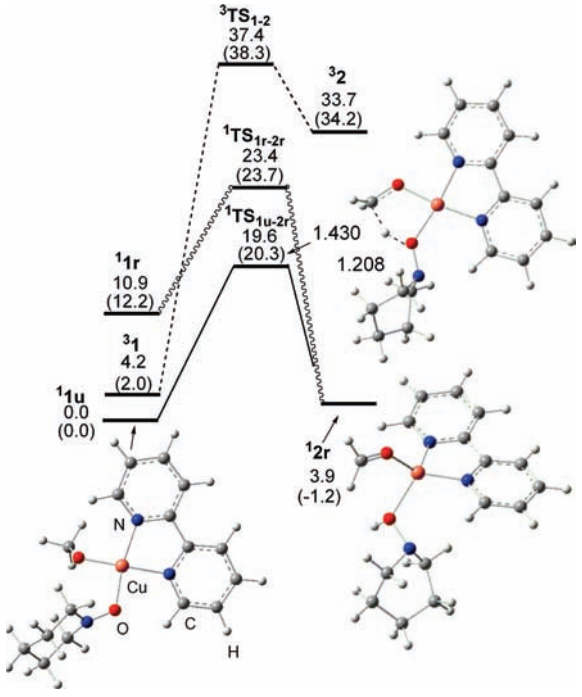

Figure 1. Calculated energy profile and optimized geometries for the H atom abstraction step. The dashed line represents triplet spin state; solid line represents open shell singlet spin state; wavy line represents restricted singlet spin state. The values are from solution, whereas those in parentheses are from the gas phase.

estimated from the following equation (based on the transition state theory)[31]

$$K = \frac{k_B T}{h} \exp(-\Delta G/RT)$$

where h is Planck's constant, k_B is Boltzmann constant, and R is the gas constant. The estimated experimental barrier height for benzyl alcohol oxidation reaction at 298.15K is 18.3 kcal/mol, which is close to the calculated barrier height 19.6 kcal/mol, demonstrating that Sheldon's mechanism is reasonable.

(27) Bassan, A.; Blomberg, M. R. A.; Siegbahn, P. E. M.; Que., L., Jr *J. Am. Chem. Soc.* **2002**, *124*, 11056.
(28) (a) Schröder, D.; Shaik, S.; Schwarz, H. *Acc. Chem. Res.* **2000**, *33*, 139and references therein;. (b) Comba, P.; Knoppe, S.; Martin, B.; Rajaraman, G.; Rolli, C.; Shapiro, B.; Stork, T. *Chem.—Eur. J.* **2008**, *14*, 344.
(29) (a) Hirao, H.; Kumar, D.; Thiel, W.; Shaik, S. *J. Am. Chem. Soc.* **2005**, *127*, 13007. (b) Cohen, S.; Kozuch, S.; Hazan, C.; Shaik, S. *J. Am. Chem. Soc.* **2006**, *128*, 11028. (c) Derat, E.; Shaik, S. *J. Am. Chem. Soc.* **2006**, *128*, 8185. (d) Kumar, D.; de Visser, S. P.; Shaik, S. *Chem.—Eur. J.* **2005**, *11*, 2825. (e) Meunier, B.; de Visser, S. P.; Shaik, S. *Chem. Rev.* **2004**, *104*, 3947.
(30) Himo, F.; Eriksson, L. A.; Maseras, F.; Siegbahn, P. E. M. *J. Am. Chem. Soc.* **2000**, *122*, 8031.
(31) Hirao, H.; Que, L., Jr; Nam, W.; Shaik, S. *Chem.—Eur. J.* **2008**, *14*, 1740.

Scheme 3. Proposed Catalytic Mechanisms for the TEMPO Regeneration

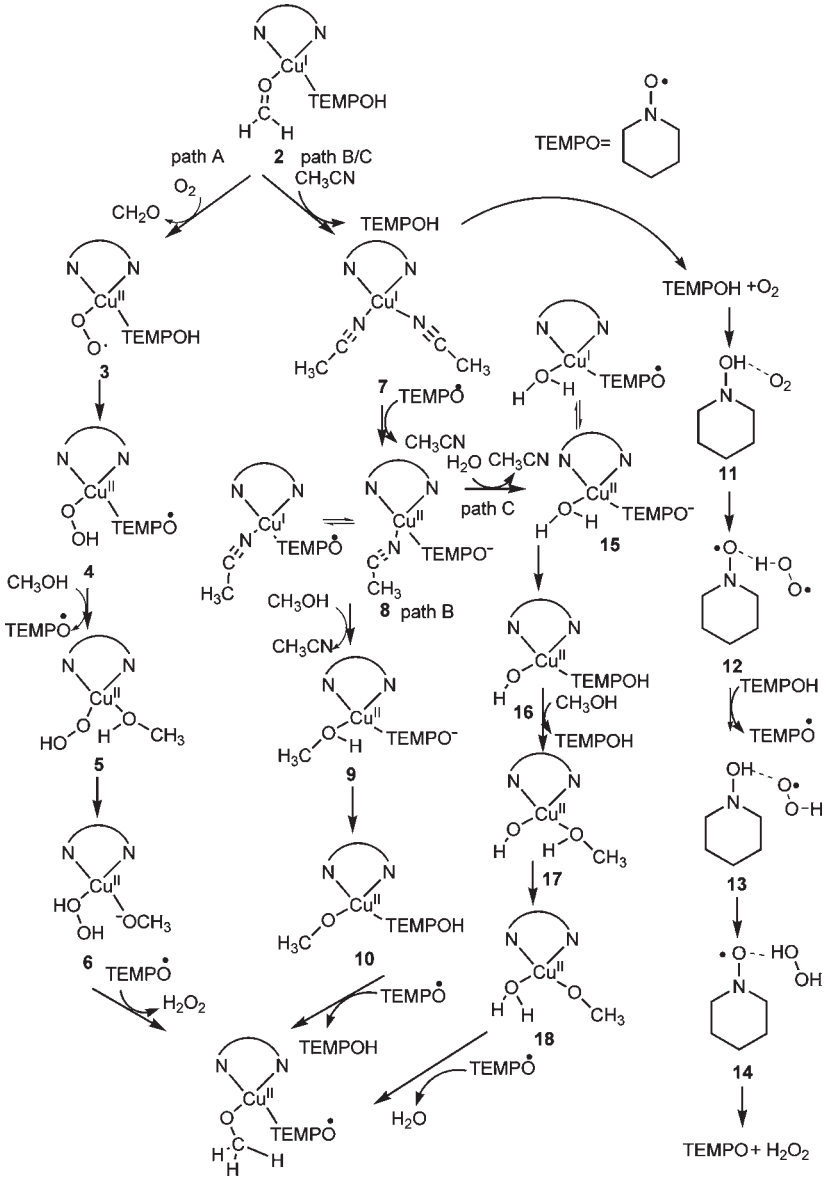

For the H atom abstraction product **2**, the unrestricted singlet ^{1}**2u** was converged to restricted closed shell singlet ^{1}**2r** during the geometry optimization. The spin densities in the restricted singlet ^{1}**2r** on all atoms are zero, indicating the (TEMPOH)(CH_2O)Cu^I(bipy) character. Thus, from ^{1}**1u** to ^{1}**2r**, product CH_2O is generated, coupled with the formation of TEMPOH.

To see if H_2O is directly involved in the catalytic reaction, a H_2O molecule was added to the studied model system. The obtained energy barrier for the H atom abstraction with water molecule is 22.1 kcal/mol, 2.5 kcal/mol higher than 19.6 kcal/mol (without water participation). This energy difference is within the B3LYP error limits (3−5 kcal/mol). Thus, our calculations suggest that the water molecule does not participate the reaction on the H atom abstraction step.

2. TEMPO Regeneration. After the TEMPOH formation, TEMPOH should be oxidized back to TEMPO to restart the catalytic cycle. In this process, three different pathways (path A, path B and path C) were proposed (Scheme 3). In path A, O_2 molecule coordinates to the Cu^I ion to form the Cu^{II}−$OO\cdot^-$ species. This species then abstracts the H atom from TEMPOH to produce TEMPO. In paths B and C, the O_2 molecule oxidizes TEMPOH directly to TEMPO (Scheme 3, process **11** → **14**). The newly formed TEMPO assists the oxidation of Cu^I to Cu^{II}. The difference between path B and C is that in path B, alcohol provides the proton to $TEMPO^-$ to produce the TEMPOH, whereas the proton is provided by H_2O in path C.

2.1. Path A. The energy profile and optimized structures are given in Figure 2. From ^{1}**2r**, the O_2 molecule replaces formaldehyde to coordinate to the Cu^I ion generating ^{3,1}**3**. On the basis of experimental and theoretical studies,[32]

(32) (a) Aboelella, N. W.; Kryatov, S. V.; Gherman, B. F.; Brennessel, W. W.; Young, V. G.; Sarangi, R.; Rybak-Akimova, E. V.; Hodgson, K. O.; Hedman, B.; Solomon, E. I.; Cramer, C. J.; Tolman, W. B. *J. Am. Chem. Soc.* **2004**, *126*, 16896. (b) Chen, P.; Solomon, E. I. *J. Am. Chem. Soc.* **2004**, *126*, 4991. (c) Schatz, M.; Raab, V.; Foxon, S. P.; Brehm, G.; Schneider, S.; Reiher, M.; Holthausen, M. C.; Sundermeyer, J.; Schindler, S. *Angew. Chem., Int. Ed.* **2004**, *43*, 4360. (d) Prigge, S. T.; Eipper, B. A.; Mains, R. E.; Amzel, L. M. *Science* **2004**, *304*, 864.

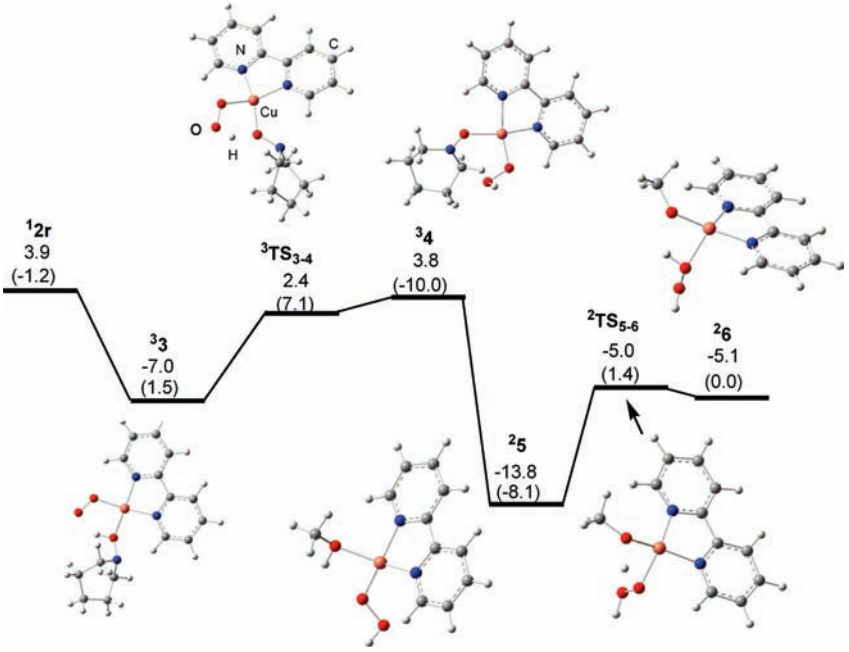

Figure 2. Calculated energy profile and optimized geometries for path A in the TEMPO regeneration process. The values are from solution, whereas those in parentheses are from the gas phase.

the side-on and end-on fashion isomers were optimized for ^{3,1}**3**. Our calculations indicate that the side-on fashion was converged to the end-on fashion during the optimization process. Thus, ^{1,3}**3** has the end-on character. In ^{3}**3** (^{1}**3**), the spin densities are 0.49 (0.53) on the Cu center, 1.26 (−0.79) on O_2 species, and 0.25 (0.26) on bipy. The small fraction of the spin density on bipy comes from the spin delocalization of the Cu center. Thus, ^{3,1}**3** has the Cu^{II}−$OO\cdot^{-}$ character. The only difference between ^{3}**3** and ^{1}**3** is that two unpaired electrons in ^{3}**3** are ferromagnetically coupled, while for ^{1}**3**, they are antiferromagnetically coupled. In addition, because ^{3}**3** is 20.6 kcal/mol lower in energy compared to ^{1}**3**, only the triplet state surface is discussed for the process **3** → **4**. In the process **3** → **4**, the reaction is endothermic by 10.8 kcal/mol (Figure 2). In ^{3}**4**, the spin densities are 0.56 on the Cu center, 0.22 on O_2 species, 0.97 on TEMPO, and 0.25 on bipy. This indicates that ^{3}**4** has the TEMPO-Cu^{II}−HOO^{-} character. Thus, the process **3** → **4** could be described as the H atom migration from TEMPOH to $OO\cdot^{-}$ species giving $^{-}$OOH species. In the process **4** → **5**, another methanol replaces TEMPO binding to the Cu center and provides a proton to the HOO^{-} group. It results in the formation of H_2O_2. Finally, another TEMPO replaces H_2O_2 to regenerate **1**. H_2O_2 could be finally reduced to H_2O in the basic environment.

2.2. Path B. The energy profile and optimized structures are given in Figure 3. From ^{1}**2r**, two CH_3CN solvent molecules replace formaldehyde and TEMPOH generating ^{1}**7**. The reaction is exothermic by 23.9 kcal/mol (in solution) in the process ^{1}**2r** → ^{1}**7**. The energy for ^{1}**7** is −20.0 kcal/mol relative to ^{1}**1u**. It seems that ^{1}**7** is very stable. This shows that the coordination of CH_3CN to Cu^{I} stabilizes the Cu^{I} species, which is consistent with the experimental conjecture.[10] After the formation of ^{1}**7**, in order to regenerate **1**, TEMPOH and Cu^{I} should be oxidized back to TEMPO and Cu^{II}. Initially, O_2 molecule oxidizes TEMPOH to TEMPO in the process **11** → **14** (Scheme 3). Subsequently, the newly formed TEMPO replaces one CH_3CN molecule to form **8**, which is in the doublet spin state. Inspection of the structure ^{2}**8**, TEMPO is coordinated to the Cu center in the η^2-*O*,*N*-fashion. In ^{2}**8**, the spin densities are 0.35 on the Cu center, 0.51 on TEMPO group, and 0.14 on bipy. The spin distribution is an indicative of the formation of the resonance structure Cu^{I}-TEMPO ↔ Cu^{II}-$TEMPO^{-}$. This means that some TEMPO radicals were reduced to $TEMPO^{-}$. From ^{2}**8**, a methanol molecule replaces CH_3CN generating ^{2}**9**. In ^{2}**9**, the spin densities are 0.51 on Cu center, 0.38 on TEMPO group, and 0.11 on bipy. The spin density on TEMPO and bipy can be traced to the electron delocalization from the Cu center. This indicates the formation of Cu^{II}-$TEMPO^{-}$. The proton then transfers from methanol to $TEMPO^{-}$ to form ^{2}**10** (CH_3O^{-}-Cu^{II}-TEMPOH). Finally, TEMPO replaces TEMPOH to regenerate **1**.

2.3. Path C. The energy profile and optimized structures are given in Figure 4. Reaction steps (**2** → **7** → **8**) and (**11** → **14**) in path C are the same to those in path B (Scheme 3 and Figure 3). From ^{2}**8**, a H_2O molecule replaces a CH_3CN molecule generating ^{2}**15**. The spin distribution for ^{2}**15** (0.41 on the Cu center, 0.48 on TEMPO group, and 0.11 on bipy) indicates the formation of the resonance structure Cu^{I}-TEMPO ↔ Cu^{II}-$TEMPO^{-}$. Then, the proton migrates from H_2O to $TEMPO^{-}$ group giving ^{2}**16** ($^{-}$OH-Cu^{II}-TEMPOH). In the following steps, methanol replaces TEMPOH forming ^{2}**17** ($^{-}$OH-Cu^{II}-CH_3OH). In the process ^{2}**17** → ^{2}**18**, the proton migrates from methanol to $^{-}$OH species giving H_2O. Finally, TEMPO replaces H_2O to coordinate to the Cu center to regenerate **1**.

2.4. Explanation of Experimental Observation. Experimentally, it has been observed that the concentration

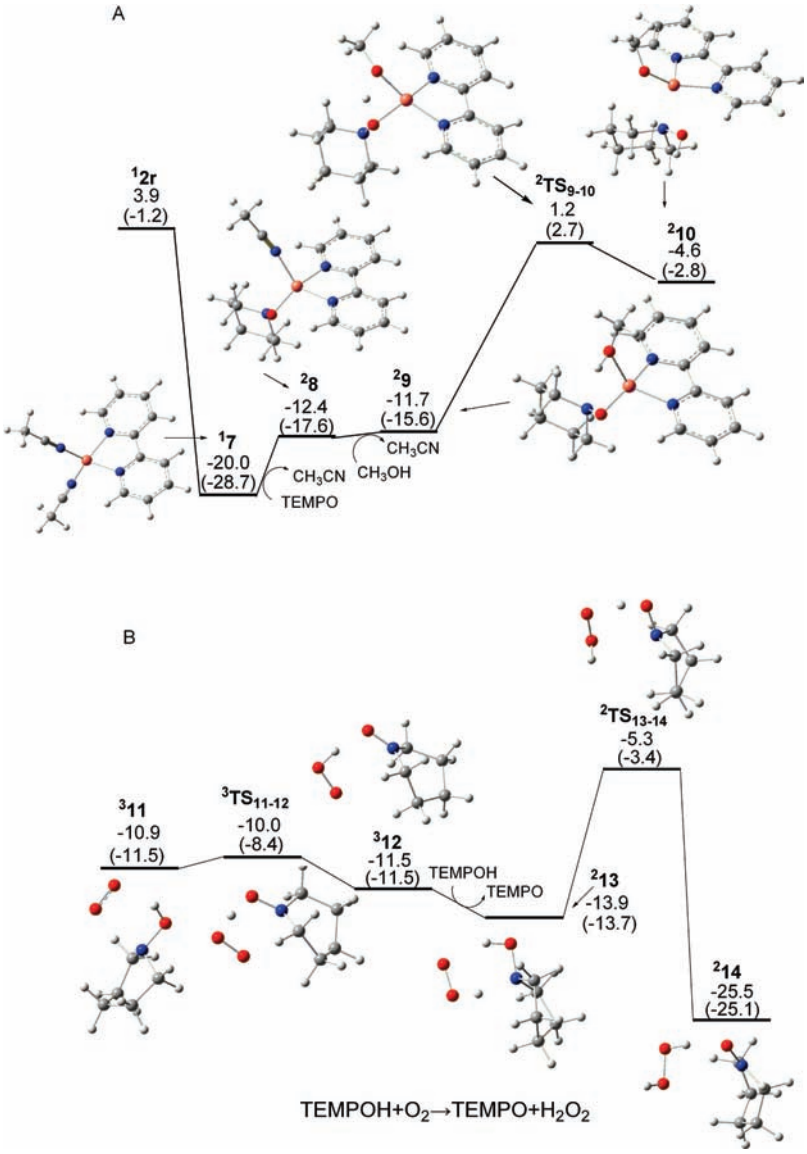

Figure 3. Calculated energy profile and optimized geometries for path B in the TEMPO regeneration process. (A) $Cu^I \rightarrow Cu^{II}$ process (B) TEMPOH → TEMPO process. The values are from solution, whereas those in parentheses are from the gas phase.

of TEMPO is constant during the course of the reaction and dramatically drops when all the substrate is consumed.[10] Thus, this observation is closely related to the TEMPO regeneration and the alcohol concentration. In the TEMPO regeneration, the proposed three paths (A, , and C) are energetically competitive. In the following, we will analyze the steps associated with the alcohol involvement in the three paths for the TEMPO regeneration i.e., **3** → **6** (path A, Figure 2), **8** → **10** (path B, Figure 3) and **16** → **18** (path C, Figure 4).

For path A, alcohol was involved in the process **4** → **5** (the alcohol molecule replaces TEMPO). If alcohol is fully consumed, the process **4** → **5** will be stopped. This would give the final product **4**. Because **4** has the TEMPO-Cu^{II}−HOO^- character (see above discussion), in which TEMPOH is oxidized to TEMPO in **4**, TEMPO will be constant even if the alcohol was consumed completely, in disagreement with the experimental observation.[10]

For path B, alcohol is used to replace CH_3CN in the process **8** → **9**. If alcohol is fully consumed, the process **8** → **9** will be terminated and gives the final product **8**. **8** has the resonance structure Cu^I-TEMPO↔ Cu^{II}-$TEMPO^-$. Thus, some TEMPO radicals can be reduced to $TEMPO^-$, in agreement with the experimental observation that TEMPO concentration change is due to the presence of $TEMPO^-$.

For path C, alcohol replaces TEMPOH (**16** → **17**) to form **17** with the (CH_3OH)-Cu^{II}-OH character. If alcohol is fully consumed, the process **16** → **17** will be stopped and give the final product **16** (TEMPOH-Cu^{II}−OH). The newly formed TEMPOH will be oxidized to TEMPO via the process **11** → **14** (Scheme 3). Thus, similar to path A, TEMPO will be constant even if the alcohol was fully consumed. That is, the fully consumed alcohol can not affect the TEMPO concentration.

In a word, among the three paths, only path B could explain the experimental observation.

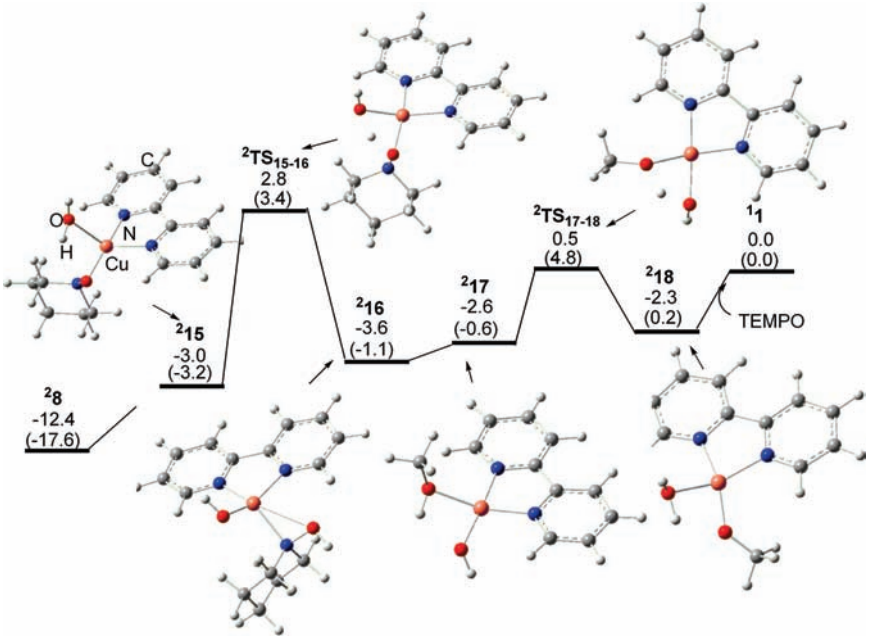

Figure 4. Calculated energy profile and optimized geometries for path C in the TEMPO regeneration process. The values are from solution, whereas those in parentheses are from the gas phase.

Conclusions

The reaction mechanisms of the alcohol oxidation catalyzed by Cu^{II}-TEMPO have been performed by use of density functional method B3LYP. The catalytic cycle consists of two parts, namely, alcohol oxidation and TEMPO regeneration. For the alcohol oxidation, two mechanisms were proposed, i.e., Semmelhack's mechanism and Sheldon's mechanism. According to our calculations, Sheldon's mechanism is preferred. The rate-determining step is the hydrogen atom transfer process in the alcohol oxidation. The calculated overall reaction barrier is 19.6 kcal/mol, which is very close to the estimated experimental barrier height 18.3 kcal/mol. For the TEMPO regeneration, three possible pathways are proposed (A, B, and C). and they are competitive in energy. By comparing with the experimental observation that the concentration of TEMPO is constant during the course of the reaction and dramatically drops when all the substrate is consumed, only path B is favored. H_2O does not directly involve in the reaction cycle in the H abstraction step. CH_3CN coordinated to the Cu^I ion stabilizing the Cu^I species, supporting the experimental conjecture.

Acknowledgment. The authors thank the National Natural Science Foundation of China for financial support (Grants 90922015, 20921002, 20831004).

Supporting Information Available: Table S1 contains the Cartesian coordinates of all the structures considered in this work from the B3LYP optimized geometries (PDF).This material is available free of charge via the Internet at http://pubs.acs.org.